

# Interactions of TiO<sub>2</sub> Nanoparticles with Ingredients from Modern Lifestyle Products and Their Effects on Human Skin Cells

Mark Geppert, Alexandra Schwarz, Lea Maria Stangassinger, Susanna Wenger, Lisa Maria Wienerroither, Stefanie Ess, Albert Duschl, and Martin Himly



Cite This: *Chem. Res. Toxicol.* 2020, 33, 1215–1225



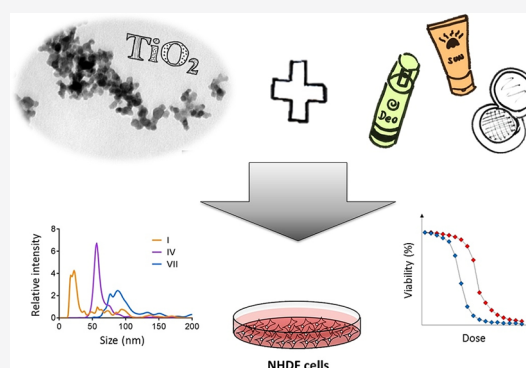
Read Online

ACCESS |

Metrics & More

Article Recommendations

**ABSTRACT:** The number of consumer products containing nanoparticles (NPs) experienced a rapid increase during the past decades. However, most studies of nanosafety have been conducted using only pure NPs produced in the laboratory, while the interactions with other ingredients in consumer products have rarely been considered so far. In the present study, we investigated such interactions—with a special focus on modern lifestyle products (MLPs) used by adolescents. An extensive survey was undertaken at different high schools all over Austria to identify MLPs that either contain NPs or that could come easily in contact with NPs from other consumer products (such as TiO<sub>2</sub> from sunscreens). Based on the results from a survey among secondary schools students, we focused on ingredients from Henna tattoos (2-hydroxy-1,4-naphthoquinone, HNQ, and *p*-phenylenediamine, PPD), fragrances (butylphenyl methylpropional, known as Lilial), cosmetics and skin-care products (four different parabens). As a cellular model, we decided to use neonatal normal human dermal fibroblasts (nNHDF), since skin contact is the main route of exposure for these compounds. TiO<sub>2</sub> NPs interacted with these compounds as evidenced by alterations in their hydrodynamic diameter observed by nanoparticle tracking analysis. Combinations of TiO<sub>2</sub> NPs with the different MLP components did not show altered cytotoxicity profiles compared to MLP components without TiO<sub>2</sub> NPs. Nevertheless, altered cellular glutathione contents were detected after incubation of the cells with Lilial. This effect was independent of the presence of TiO<sub>2</sub> NPs. Testing mixtures of NPs with other compounds from consumer products is an important approach to achieve a more reliable safety assessment.



## 1. INTRODUCTION

Titanium dioxide nanoparticles (TiO<sub>2</sub> NPs) are among the most produced types of nanoparticles, with annual production volumes of more than 3000 tons per year.<sup>1,2</sup> Substantial effort has been undertaken to assess the safety of TiO<sub>2</sub> NPs (and NPs in general); however, most of these studies use pristine NPs synthesized in the lab and do not consider mixtures of NPs with other compounds present in consumer products. Since TiO<sub>2</sub> NPs are frequently present in sunscreens,<sup>3</sup> we focused on this particle type, as it is likely to come in contact with chemicals from modern lifestyle products (MLPs) and rise to coexposure *via* the skin.

In general, the outer layer of the human skin is tough and penetration of inorganic NPs through it is very limited.<sup>4–6</sup> While most studies show that TiO<sub>2</sub> NPs do not penetrate the intact or even damaged skin,<sup>7,8</sup> a paper by Wu and co-workers showed penetration of TiO<sub>2</sub> NPs through the nondamaged skin of hairless mice.<sup>9</sup> In the latter study, increased amounts of titanium were observed in different organs such as heart, liver, spleen, and brain. Furthermore, the authors detected significant alterations in malondialdehyde and superoxide

dismutase levels in the liver of TiO<sub>2</sub> NP-exposed mice.<sup>9</sup> In a recent study on humans, Pelclova et al. detected TiO<sub>2</sub> NPs in plasma and urine samples 6–48 h after sunscreen use, demonstrating that detectable amounts of the particles can pass the protective layers of the skin.<sup>10</sup>

In addition to *in vivo* studies, several *in vitro* approaches have been undertaken to study the effects of TiO<sub>2</sub> NPs on skin cells. Wright and colleagues studied the effects of differently sized TiO<sub>2</sub> NPs on a human keratinocyte cell line (HaCaT) and concluded that all forms of TiO<sub>2</sub> NPs tested lead to a dose-dependent increase in superoxide production, caspase 8 and 9 activity, and apoptosis.<sup>11</sup> In another study by Crosera et al., the authors showed that TiO<sub>2</sub> NPs induce cytotoxic effects on HaCaT cells with EC<sub>50</sub> concentrations in the range 10<sup>−4</sup>–10<sup>−5</sup>

Special Issue: Future Nanosafety

Received: October 21, 2019

Published: February 24, 2020



mol/L.<sup>7</sup> An earlier study by Pan and co-workers showed that TiO<sub>2</sub> NPs are taken up by primary human dermal fibroblasts and lead to a decrease in cell area, proliferation, mobility, and the ability to contract collagen.<sup>12</sup> It has to be noted that in all of these studies, pure lab-synthesized TiO<sub>2</sub> NPs were used.

In reality, the dermal encounter of TiO<sub>2</sub> NPs occurs for consumers in combination with other external stressors, such as UV light or chemicals. While combinations of TiO<sub>2</sub> NPs and UV light have been examined previously,<sup>13,14</sup> there is a lack of data on the combinatorial effects of TiO<sub>2</sub> NPs with other ingredients from consumer products, e.g., modern lifestyle products (MLPs) such as henna tattoos or certain fragrances or skin-care products. Coexposure of the skin to such MLP ingredients in combination with TiO<sub>2</sub> NPs (for example, from sunscreens) is highly likely and needs to be investigated.

Temporary black henna tattoos became fashionable during the past 15 years among adolescents and are especially applied in holiday areas such as southern European countries by street tattoo artists or at festivals and fairs.<sup>15,16</sup> While the natural orange henna pigments extracted from the plant *Lawsonia inermis* is normally considered as not dangerous, temporary black henna tattoos often contain other ingredients such as the organic compound *para*-phenylenediamine (PPD), which is known to cause hypersensitivity reactions and lead to severe skin damage.<sup>17</sup> In addition, it could be shown *in vitro* that PPD induces dose-dependent cytotoxicity, oxidative stress and altered mRNA expression levels in normal human hair dermal papilla cells.<sup>18</sup> Whether a coexposure of PPD with nanoparticles can lead to enhancement of these effects has not been studied so far.

In addition to tattoos or body-paintings, the skin encounters several other chemicals, e.g., from cosmetics or fragrances. One example is the compound 3-(4-*tert*-butylphenyl)-2-methylpropanal, better known as Lilial, which is discussed to cause contact dermatitis<sup>19,20</sup> and induces dose-dependent toxicity, a decrease of cellular ATP content, and an increase of reactive oxygen species (ROS) production in HaCaT cells.<sup>21</sup> Other critical compounds of cosmetic products are the so-called parabens (esters of parahydroxybenzoic acid), which are used as preservatives in different consumer products, especially in cosmetics.<sup>22</sup> Parabens can penetrate the skin and are discussed to have estrogenic activity and even carcinogenic potential.<sup>22,23</sup> In addition, parabens have been shown *in vitro* to induce cytotoxicity and/or genotoxicity.<sup>24,25</sup>

To our knowledge, no study is available so far that investigates the combinatorial effects of TiO<sub>2</sub> NPs with one of these aforementioned substances on human skin cells. However, since the simultaneous encounter of the human skin to both, TiO<sub>2</sub> NPs, and other compounds from cosmetics, fragrances, or henna tattoos is highly likely, we decided to investigate how these combinations could interact regarding both the characteristics of the NPs and the biological response of human skin cells. We thereby focused on pairwise testing of the individual substances with/without TiO<sub>2</sub> NPs and excluded combinations of multiple substances with the NPs (except for the henna dyes, where we also tested black henna, which contained both, HNQ and PPD). This strategy was chosen since we are particularly interested in the influence of the TiO<sub>2</sub> NPs on potential harmful effects of the substances on human skin, rather than on combinations of several substances. As end points, we decided to use the classical markers for cell stress and cytotoxicity (metabolic activity, lysosomal integrity, apoptosis, oxidative stress) in order to reveal potential harmful

effects of the TiO<sub>2</sub>/MLP combinations on a basic mechanistic level. A more detailed analysis on potential allergenic or inflammatory effects (due to the substances itself or to contaminations with endotoxins or allergens) was not part of our study but will be interesting for future work in the field.

## 2. MATERIALS AND METHODS

**Materials.** Fetal bovine serum (FBS) was purchased from Biochrom (Berlin, Germany), CellTiter-Blue reagent from Promega (Madison, WI, United States), and carboxy-2',7'-dichlorodihydrofluorescein diacetate and fluorescein-conjugated Annexin V from Thermo Fisher Scientific (Waltham, MA, United States). All other chemicals were obtained from Sigma-Aldrich (Vienna, Austria) at high purity. This includes the tested ingredients from the modern lifestyle products (MLP ingredients), which were purchased as pure chemicals (>96% purity, details see Table 1).

**Table 1. Ingredients from Modern Lifestyle Products (MLPs) Used for Investigation of Their Effects on Human Skin Cells in Combination with TiO<sub>2</sub> NPs<sup>a</sup>**

compound	purity (%)	origin	concentration (mM)
2-hydroxy-1,4-naphthoquinone (HNQ)	≥97	henna tattoos	2
<i>para</i> -phenylenediamine (PPD)	≥98	black Henna tattoos, hair tinting lotions	0.5
HNQ + PPD	≥97 ≥98	black Henna tattoos	0.25 + 0.25
3-(4- <i>tert</i> -butylphenyl)-2-methylpropanal (Lilial)	≥96	fragrance used in different cosmetics and skin-care products	0.125
methyl parabene (MP)	≥99	preservative in skin-care products	2
ethyl parabene (EP)	≥99	preservative in skin-care products	1
propyl parabene (PP)	≥99	preservative in skin-care products	0.5
butyl parabene (BP)	≥99	preservative in skin-care products	0.25

<sup>a</sup>The substances were selected from an extensive survey of the use of different MLPs by 252 adolescents in high schools in Austria. Compounds were ordered from Sigma-Aldrich (Vienna, Austria) with the indicated purities. The concentrations given in the last column reflect the concentrations used for the experiments in the present study and are determined as sub-toxic concentrations from dose-response analysis (see Figure 4 and Table 3).

**Nanoparticles.** Titanium dioxide nanoparticles (TiO<sub>2</sub> NPs) were prepared using a metal organic chemical vapor synthesis approach, as described previously.<sup>26–28</sup> To disperse TiO<sub>2</sub> NPs in water, 2 mg of particles were suspended in 2 mL of H<sub>2</sub>O in an Eppendorf cup, vortexed, and subsequently sonicated for 30 min using the UP200St equipped with an S26d2 sonotrode (Hielscher, Teltow, Germany).

**Modern Lifestyle Products.** Different modern lifestyle products (MLPs) were chosen to study their interactions and combinatorial effects with TiO<sub>2</sub> NPs. The decision for the products and their ingredients tested relies on an extensive survey that was performed on different high schools all over Austria. In detail, data collection was carried out in a two-step process containing (i) a theme processing at school and (ii) an individual online questionnaire. The online survey was divided into the categories, (a) cosmetics, (b) food products, (c) fitness and hobby, (d) party, and (e) others. Test persons should name products of daily use for each category, their common purpose, as well as unusual handling of MLPs. Data evaluation was conducted based on the qualitative content analysis of Mayring, a systematic method used to analyze linguistic material and texts.<sup>29</sup> In accordance

with Mayring, a process model was developed to split the data analysis into single steps and to generate a transparent and traceable structure.

**Characterization of TiO<sub>2</sub> NPs and Their Interactions with MLP Ingredients.** TiO<sub>2</sub> NPs and their interactions with MLP ingredients were investigated using nanoparticle tracking analysis (NTA).<sup>30</sup> This method allows for the determination of hydrodynamic particle sizes in dispersion with the advantage of a higher resolution of multiple peaks in polydisperse NP samples compared to standard DLS methods.<sup>30</sup> In addition, NTA is able to estimate particle numbers in samples. In order to determine NP–MLP-ingredient interactions, a mixture of 0.1 mg/mL TiO<sub>2</sub> NPs with 0.1 mg/mL of the respective MLP ingredient was prepared and incubated for 60 min on a rotator to prevent sedimentation. The sample was then diluted with pure H<sub>2</sub>O by a factor of 100 and injected into the measurement cell of the NanoSight LM10 (Malvern Instruments, Malvern, United Kingdom). For measurement, five videos of each 30 s duration were recorded and analyzed according to the manufacturer's instructions. Three independent measurements were performed on individually prepared samples.

**Cell Culture.** Neonatal normal human dermal fibroblasts (nNHDF) cells were purchased from Clonetics (Walkersville, MD, United States) and cultured in Dulbecco's modified Eagle's Medium (DMEM) supplemented with 10% FBS, 100 units/mL Penicillin, 100 µg/mL Streptomycin, 2 mM L-Glutamine, and 5 mL of Nonessential amino acid solution. Cells were passaged twice per week using standard sterile cell culture techniques. For incubation experiments with TiO<sub>2</sub> NPs and/or MLP ingredients, 38000 viable cells were seeded in 1 mL of culture medium per well of a 24-well plate and grown for 24 h. Cells of passage numbers between 6 and 20 were used.

**Experimental Incubation.** Cells were taken out of the incubator, and the media were aspirated using a suction pump (Vacuubrand, Wertheim, Germany). Freshly prepared solutions (500 µL) of TiO<sub>2</sub> NPs and/or MLP ingredients in the desired concentrations were added, and the cells were incubated for the desired time points. After incubation, the media were collected and the cells were washed twice with 1 mL of phosphate buffered saline (PBS) before further investigation.

**Cytotoxicity Evaluation.** The cytotoxicity of MLP ingredients in absence or presence of TiO<sub>2</sub> NPs was analyzed by measuring two different end points (CellTiter-Blue (CTB) assay and Neutral Red Uptake (NRU) assay), as described previously.<sup>31</sup>

**Apoptosis Assay.** Apoptosis was determined using the Annexin V/Propidiumiodide (PI) staining method as described in Crowley et al.,<sup>32</sup> which was slightly modified. Cells were detached from the plates with 150 µL of trypsin–EDTA solution, washed once with 500 µL of PBS and once with 500 µL of Annexin binding buffer (BB: 10 mM HEPES, 140 mM NaCl, 2.5 mM CaCl<sub>2</sub>, pH = 7.4), and then incubated for 30 min with 150 µL of BB containing 1.5 µL of FITC conjugated Annexin V antibody at room temperature in the dark. After incubation, 1 mL of BB was added and the cells were washed again with 500 µL of BB. Cells were then resuspended in 500 µL of BB containing 2 µg/mL PI, incubated at room temperature, and analyzed by flow cytometry for their fluorescence. Cells incubated with 1 µM staurosporine were used as positive control.

**Reactive Oxygen Species Assay.** Intracellular reactive oxygen species (ROS) were stained and quantified using the dye 6-carboxy-2',7'-dichlorodihydrofluorescein diacetate (DCFDA). One hour before the end of incubation of the cells with TiO<sub>2</sub> NPs and/or MLP ingredients, 5 µL of a 1 mM solution of DCFDA in DMSO was added to the media and mixed carefully. After the incubation, the cells were washed twice with PBS, detached from the plates by 150 µL of trypsin–EDTA solution, and resuspended in 500 µL of culture medium. Cell suspensions were analyzed by flow cytometry for their fluorescence (FITC channel) using the FACSCanto II flow cytometer (BD Biosciences, San Jose, CA, United States). Hydrogen peroxide (H<sub>2</sub>O<sub>2</sub>, *c* = 100 µM) was used as a positive control.

**Glutathione Assay.** Intracellular total and oxidized glutathione was determined by the earlier published Tietze method,<sup>33</sup> which was adapted to microtiter plates. Briefly, cells were lysed in 200 µL of 1%

(w/v) sulfosalicylic acid (SSA), and 10 µL of the lysates were diluted with 90 µL of H<sub>2</sub>O and subsequently mixed with 100 µL of a reaction mixture containing 0.3 mM DTNB, 0.4 mM NADPH, 1 mM EDTA, and 1 U/mL glutathione reductase in 0.1 mM sodium phosphate buffer, pH = 7.5. The absorbance at 405 nm was continuously recorded over a time frame of 10 min. Glutathione concentrations were determined by comparing the increase in absorption of samples with the increase in absorption of standards with known concentrations. In order to determine the amount of oxidized glutathione (glutathione disulfide, GSSG), the samples were pre-treated with 2-vinylpyridine (2-VP). The sample (cell lysate in SSA, 130 µL) was mixed with 5 µL of 2-VP, and the pH was subsequently adjusted to 6 using 0.2 M Tris-solution. Samples were incubated at room temperature for 60 min, and then 10 µL of the samples were assayed for glutathione, as described above.

**Determination of Protein Contents.** Cellular protein contents were determined after lysis of the cells in 200 µL of 0.5 M NaOH according to the Lowry method<sup>34</sup> using bovine serum albumin as a standard.

**Statistical Analysis.** If not stated otherwise, the data represent mean values ± standard deviation (SD) of a minimum of three experiments performed on different passages of cells with individually prepared solution of TiO<sub>2</sub> NPs and/or MLP ingredients. Analysis of significances of differences between two sets of data was performed by the unpaired *t*-test, while groups of data were analyzed using ANOVA with Bonferroni's *post hoc* test (multiple comparisons) or Dunnett's *post hoc* test (multiple comparisons to a control). A *p*-value larger than 0.05 was considered as not significant.

### 3. RESULTS

#### Identification of Modern Lifestyle Products (MLPs).

Modern lifestyle products (MLPs) used in this study were identified by an extensive survey at seven different high schools all over Austria. In detail, the data evaluation of 252 collected data sets based on the qualitative content analysis of Mayring revealed 390 MLPs in five different categories, cosmetics, fitness and hobby, food products, party, and other. Since most mentioned MLPs referred to the category of cosmetics (305 nominations), this category was further divided into different subcategories (Figure 1). More than 75% of the nominations belonged to hair-care, skin-care, or decorative cosmetics, while other products such as perfumes only represented a minority.

Since the main exposure route for the identified MLPs was the transdermal route *via* the skin (84% of the MLPs, Figure 2), we decided to focus on these products and their ingredients for the current study. Seven different substances that had been



**Figure 1.** Distribution of the surveyed modern lifestyle products (MLPs) of the category cosmetics. From 390 total MLPs mentioned in the survey, 305 belong to the category of cosmetics and distribute to the presented subcategories.

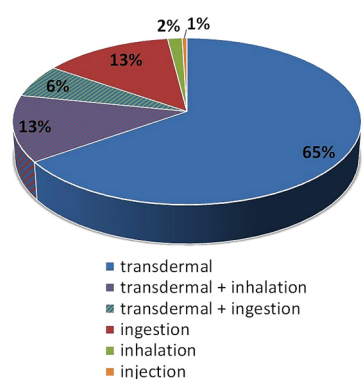


**Figure 2.** Percentage distribution of exposure routes of surveyed modern lifestyle products (MLPs).

previously shown to be of concern were selected to study their effects alone or in combination with TiO<sub>2</sub> NPs on human skin cells. These substances and their origin are listed in Table 1.

**Nanoparticles and Their Interactions with MLP Ingredients.** Anatase TiO<sub>2</sub> NPs were synthesized and characterized as previously described.<sup>31,35</sup> The primary particle size was investigated by transmission electron microscopy and was determined as  $12 \pm 3$  nm. Dispersed in water, TiO<sub>2</sub> nanoparticles tend to form small agglomerates with average diameters of  $192 \pm 3$  nm, as measured previously by dynamic light scattering.<sup>31</sup> Detailed analysis of the size distribution of the TiO<sub>2</sub> NPs by nanoparticle tracking analysis (NTA) revealed a rather bell-shaped curve with hydrodynamic diameters of around 50–250 nm for most of the particles (Figure 3). Calculations on the size distribution reveal mean, mode, and D50 values of  $130 \pm 13$ ,  $107 \pm 13$ , and  $122 \pm 12$

nm, respectively (Table 2). Pretreatment of TiO<sub>2</sub> NPs with different MLP ingredients did not lead to any significant

**Table 2.** Particle Diameters (Mean, Mode and D50 Values) and Particle Numbers of TiO<sub>2</sub> NPs after Incubation with MLP Ingredients<sup>a</sup>

	mean (nm)	mode (nm)	D50 (nm)	# of particles ( $\times 10^6$ )
control	$130 \pm 13$	$107 \pm 13$	$122 \pm 12$	$1268 \pm 542$
HNQ	$154 \pm 14$	$117 \pm 18$	$141 \pm 20$	$498 \pm 380^*$
PPD	$138 \pm 19$	$122 \pm 14$	$129 \pm 17$	$1833 \pm 93$
HNQ + PPD	$180 \pm 69$	$176 \pm 118$	$170 \pm 88$	$295 \pm 325^{**}$
Lilial	$136 \pm 5$	$117 \pm 11$	$127 \pm 6$	$552 \pm 248$
MP	$131 \pm 2$	$106 \pm 5$	$122 \pm 1$	$927 \pm 146$
EP	$132 \pm 5$	$105 \pm 8$	$122 \pm 2$	$764 \pm 92$
PP	$126 \pm 1$	$103 \pm 5$	$119 \pm 2$	$612 \pm 210$
BP	$136 \pm 18$	$111 \pm 19$	$122 \pm 12$	$748 \pm 137$

<sup>a</sup>TiO<sub>2</sub> NPs were incubated with MLP ingredients, and their size distribution was measured using NTA as shown in Figure 3. Statistical mean, mode, and D50 values as well as particle numbers were calculated. The data represent mean values  $\pm$  SD of three individual performed measurements with individual sets of particles and MLP ingredients. Stars indicate the significance of differences between control conditions (TiO<sub>2</sub> NPs only) and TiO<sub>2</sub> NPs mixed with MLP ingredients; \* $p < 0.05$ , \*\* $p < 0.01$ .

changes in their mean, mode, or D50 values; however, there was a significant reduction in detectable particle number from  $(1268 \pm 542) \times 10^6$  particles in the control condition to  $(498 \pm 380) \times 10^6$  particles in the sample incubated with HNQ and to  $(295 \pm 325) \times 10^6$  particles in the sample incubated with

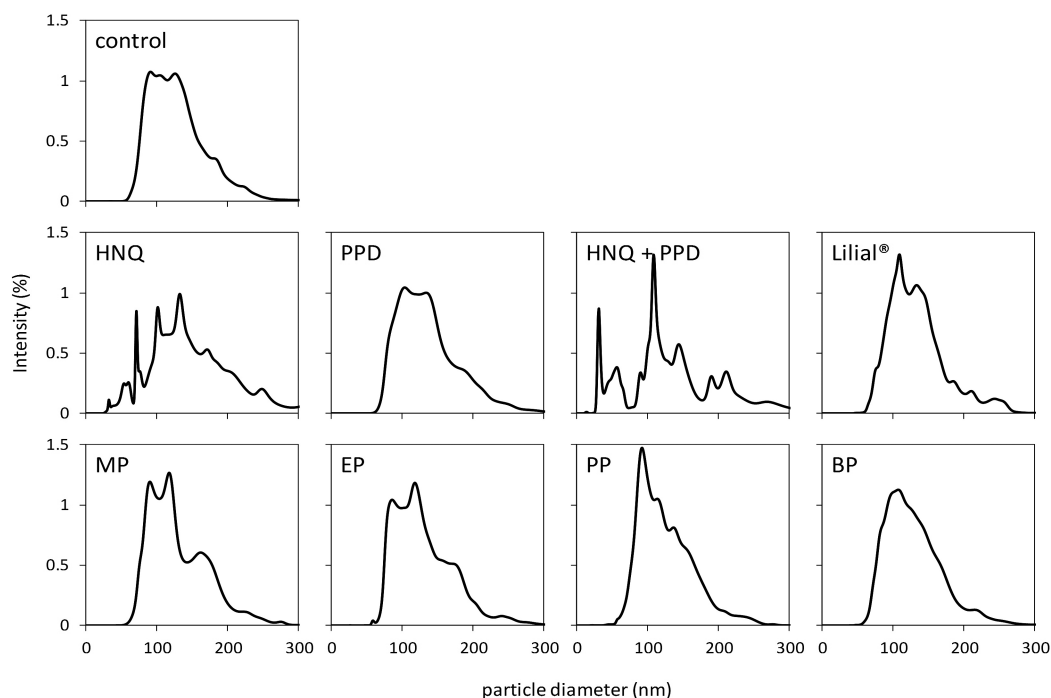


**Figure 3.** Particle size distribution curves of TiO<sub>2</sub> NPs after incubation with MLP ingredients. TiO<sub>2</sub> NPs (0.1 mg/mL) were mixed with 0.1 mg/mL of 2-hydroxy-1,4-naphthoquinone (HNQ), *para*-phenylenediamine (PPD), HNQ + PPD, Lilial, methyl parabene (MP), ethyl parabene (EP), propyl parabene (PP), or butyl parabene (BP) and incubated for 60 min on a rotator. Ten microliters of the mixtures was diluted with 990  $\mu$ L of pure water, and the particle size distribution was determined using NTA. The size distribution curves represent mean values of three experiments performed with individually prepared samples.

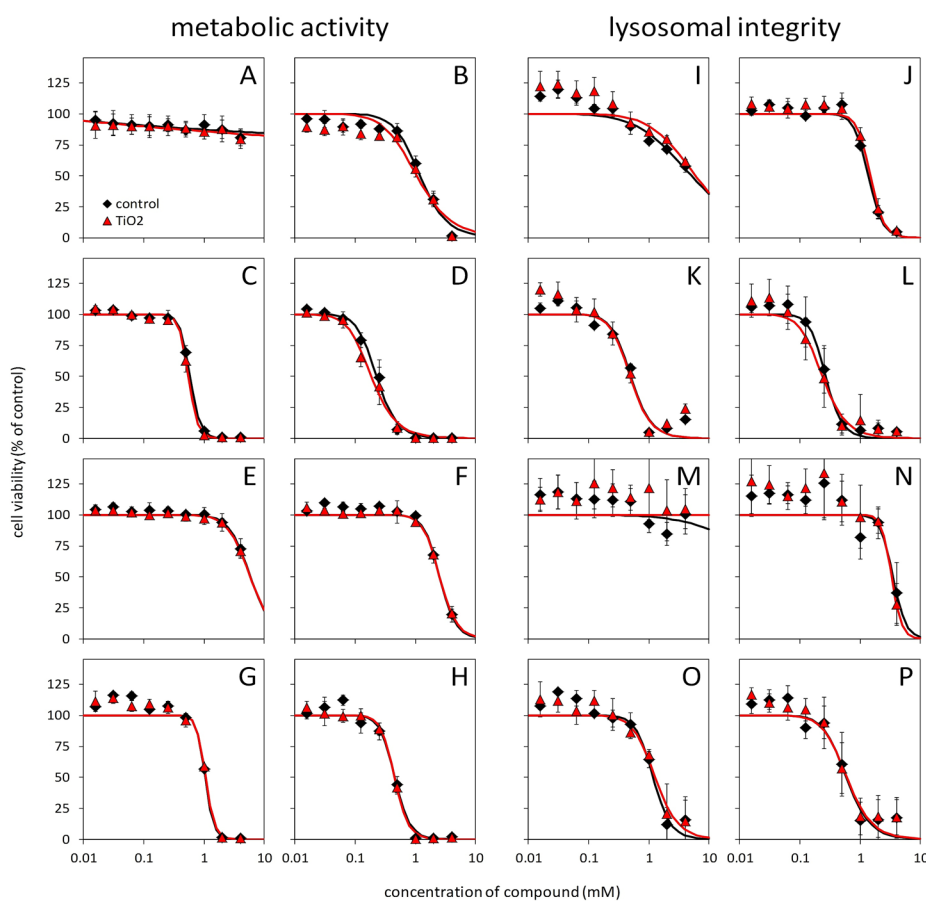


**Figure 4.** Cytotoxicity of different MLP ingredients in absence or presence of  $\text{TiO}_2$  NPs. The cells were incubated for 24 h with various concentrations of 2-hydroxy-1,4-naphthoquinone (HNQ, A, I), *para*-phenylenediamine (PPD, B, J), HNQ + PPD (C, K), Lilial (D, L), methyl parabene (E, M), ethyl parabene (F, N), propyl parabene (G, O), or butyl parabene (H, P) in absence (control) or presence ( $\text{TiO}_2$ ) of 100  $\mu\text{g}/\text{mL}$   $\text{TiO}_2$  NPs. After incubation, the cell viability was assessed by determination of the metabolic activity (CTB assay, A–H) and the lysosomal integrity (NRU assay, I–P). Cell viability is always expressed as %viability compared to control cells (treated with cell culture medium only). The data represent mean values  $\pm$  SD of three different experiments performed individually on independently prepared cultures.

HNQ and PPD (Table 2). These alterations in total detectable particle number are also reflected in the size distribution curves, which show strong differences in their appearance in these two conditions compared to the control or to samples incubated with the other MLP ingredients (Figure 3).

**Cytotoxicity of MLP Ingredients.** In order to determine the cytotoxicity of the MLP ingredients and to reveal the influence of  $\text{TiO}_2$  NPs, a detailed dose–response analysis was performed using nNHDF cells as a model. Incubation of the cells for 24 h with increasing concentrations (0.125–4 mM) of MLP ingredients revealed typical sigmoidal dose–response curves for most of the substances in both, absence or presence of 100  $\mu\text{g}/\text{mL}$   $\text{TiO}_2$  NPs (Figure 4). Only for HNQ (Figure 4A) and for MP (Figure 4M), no sigmoidal-shaped dose–response curves were obtained, indicating that for these substances, even the highest concentration tested did not lead to a substantial alteration of the respective readout (metabolic activity, Figure 4A, or lysosomal integrity, Figure 4M). For all substances tested, no influence of the presence of 100  $\mu\text{g}/\text{mL}$   $\text{TiO}_2$  NPs was detectable. This is also reflected in the EC50 values, which were calculated from the dose–response curves using a 4-parameter nonlinear regression analysis (Table 3). EC50 concentrations for the different MLP ingredients were between  $0.27 \pm 0.07$  mM (Lilial) and  $>10$  mM (HNQ) and did not significantly alter when  $\text{TiO}_2$  NPs were present.

**Table 3.** EC50 Values Determined on Exposure of nNHDF Cells with Different Compounds in Absence (Control) or Presence ( $\text{TiO}_2$ ) of 100  $\mu\text{g}/\text{mL}$   $\text{TiO}_2$  NPs for 24 h

compound	end point	EC50 (mM)	
		control	$\text{TiO}_2$
HNQ	metabolic activity	>10	>10
	lysosomal integrity	$5.28 \pm 1.09$	$6.18 \pm 0.85$
PPD	metabolic activity	$1.19 \pm 0.17$	$1.06 \pm 0.20$
	lysosomal integrity	$1.36 \pm 0.05$	$1.48 \pm 0.17$
HNQ + PPD	metabolic activity	$0.58 \pm 0.02$	$0.54 \pm 0.04$
	lysosomal integrity	$0.5 \pm 0.03$	$0.48 \pm 0.07$
Lilial	metabolic activity	$0.23 \pm 0.05$	$0.19 \pm 0.05$
	lysosomal integrity	$0.27 \pm 0.07$	$0.25 \pm 0.09$
MP	metabolic activity	$9.28 \pm 7.28$	$6.31 \pm 2.11$
	lysosomal integrity	>10	>10
EP	metabolic activity	$2.55 \pm 0.26$	$2.55 \pm 0.03$
	lysosomal integrity	$3.54 \pm 0.86$	$3.34 \pm 0.6$
PP	metabolic activity	$1.04 \pm 0.02$	$1.05 \pm 0.02$
	lysosomal integrity	$1.27 \pm 0.34$	$1.44 \pm 0.49$
BP	metabolic activity	$0.45 \pm 0.05$	$0.45 \pm 0.03$
	lysosomal integrity	$0.69 \pm 0.42$	$0.7 \pm 0.35$

For a more detailed investigation of the effects of MLP ingredients in combination with  $\text{TiO}_2$  NPs, subtoxic

concentrations of the MLP ingredients were chosen. These concentrations are in the range of the EC<sub>20</sub> values (i.e., ~80% cell viability) and are depicted in Table 1. In order to study the mechanism of potential loss in cell viability in more detail, a combined apoptosis/necrosis assay was performed using flow cytometry after staining of the cells with the FITC-labeled Annexin V antibody and the dye Propidiumiodide (PI). Differentiation between viable, apoptotic, and necrotic cells was achieved by applying a 4-quadrant gating strategy using a threshold of >95% viable cells in the negative control (NC, Figure 5). As expected from the chosen concentrations of MLP

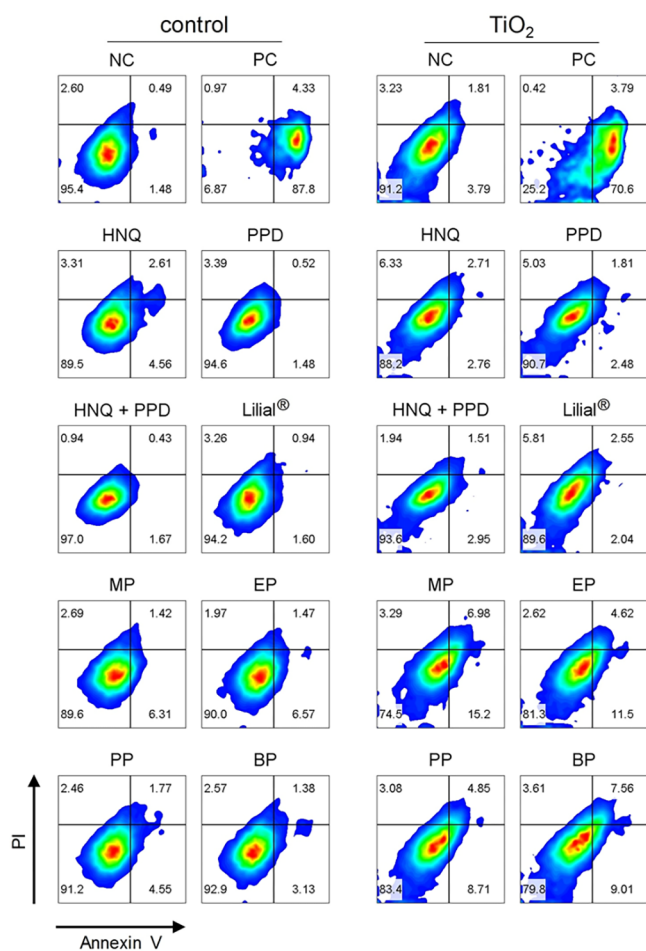


**Figure 5.** Apoptosis assay of different MLP ingredients in absence or presence of TiO<sub>2</sub> NPs. nNHDF cells were incubated for 24 h with different MLP ingredients (for concentrations see Table 1) in absence (control) or presence (TiO<sub>2</sub>) of 100 μg/mL TiO<sub>2</sub> NPs. After incubation, apoptosis was determined using FITC-labeled Annexin V, while necrosis was determined using Propidiumiodide (PI). The data show the results from flow cytometry of a representative experiment reproduced two times with comparable results. NC, negative control; PC, positive control (1 μM staurosporine).

ingredients, the amount of viable cells was >80% for most of the substances tested, while only two of the parabens (MP, BP) lead to slightly reduced numbers of viable cells (74.5% and 79.8%, respectively). Quantification of the fluorescence data on both channels (FITC and PI) revealed that neither the differences between the NC and the MLP-exposed cells nor the differences between control and TiO<sub>2</sub> NP-exposed cells reach the level of significance (Figure 6). Only in the case of PPD together with the TiO<sub>2</sub> NPs was a significant difference in

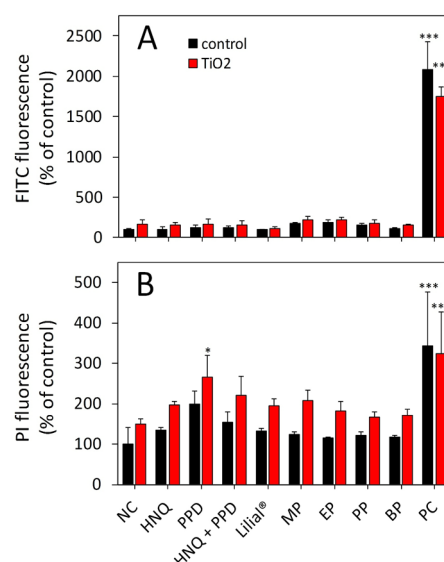


**Figure 6.** Quantification of apoptosis and necrosis in nNHDF cells after incubation with MLP ingredients in absence or presence of TiO<sub>2</sub> NPs. The cells were incubated for 24 h with different MLP ingredients (for concentrations see Table 1) in absence (control) or presence (TiO<sub>2</sub>) of 100 μg/mL TiO<sub>2</sub> NPs and assayed for apoptosis using FITC-labeled Annexin V (A) and necrosis using Propidiumiodide (B). The bar charts show median fluorescence intensities ± SD from flow cytometry data (see Figure 5) given as percentage of negative control (NC) of three independently performed experiments. Stars indicate the significance of differences of exposed conditions compared to the negative control (NC); \**p* < 0.05, \*\*\**p* < 0.001. PC: positive control (1 μM staurosporine).

PI fluorescence compared to the control observed. In addition, there is a clear trend that TiO<sub>2</sub> NP-exposed cells always show a higher PI fluorescence than control cells (Figure 6B).

**Reactive Oxygen Species Assay.** To determine the potential of the MLP ingredients and/or TiO<sub>2</sub> NPs to induce oxidative damage, a staining for reactive oxygen species (ROS) was performed and analyzed by flow cytometry using a double detection method (side-scatter vs. fluorescent signal, Figure 7) and a fluorescent signal quantification method (Figure 8). There was no severe elevation in the DCFDA signal in any of the exposed conditions, with or without TiO<sub>2</sub> NPs, indicating no substantial amount of ROS formed in the cells. Only the positive control (PC: 100 μM H<sub>2</sub>O<sub>2</sub>) showed a slight but significant increase in the DCFDA signal (Figure 8), demonstrating that the ROS assay was functional in nNHDF cells—even though with a low sensitivity. Nevertheless, a significant difference between positive and negative control was demonstrated, so DCFDA assay was suitable for ROS determination in our setting. The discrepancies between the amount of “ROS positive” events (gating strategy, Figure 7) and median fluorescence intensities (Figure 8) are thus a result of applying two different quantification methods. In addition to the fluorescence signal of the dye, also the side scatter signal (SSC) was recorded as an indicator for cell granularity and, hence, particle accumulation.<sup>36</sup> The data show that there was a significant increase in SSC for all the conditions containing TiO<sub>2</sub> NPs compared to the controls, indicating TiO<sub>2</sub> NP accumulation in cells independent of the MLP ingredients.

**Cellular Glutathione Content.** As an additional marker for cellular (oxidative) stress, the total cellular glutathione (GSH) content as well as the amount of oxidized glutathione

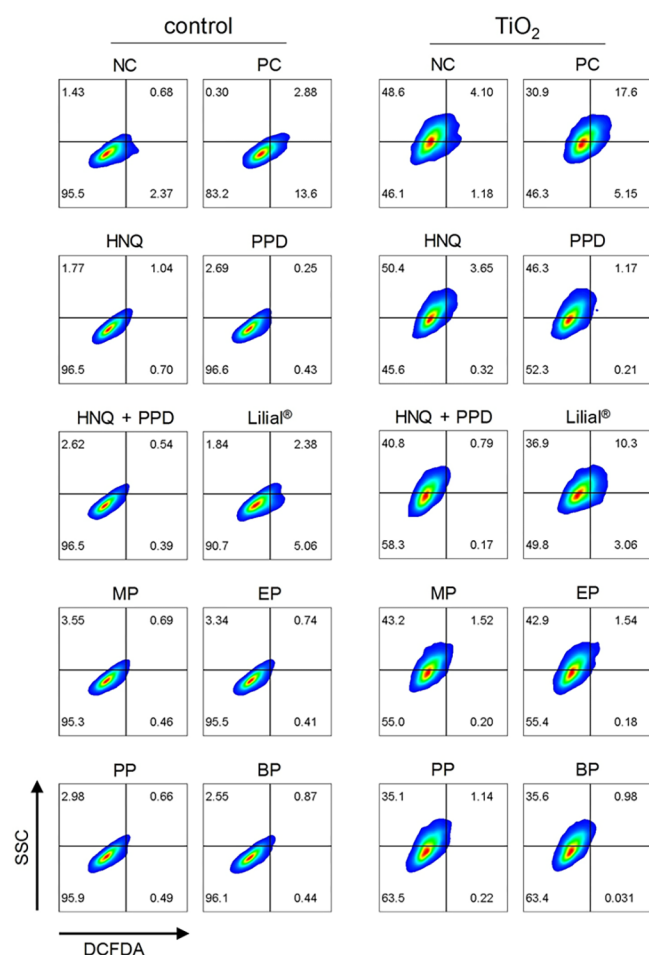


**Figure 7.** Reactive oxygen species (ROS) assay of different MLP ingredients in absence or presence of TiO<sub>2</sub> NPs. nNHDF cells were incubated for 4 h with different MLP ingredients (for concentrations see Table 1) in absence (control) or presence (TiO<sub>2</sub>) of 100 μg/mL TiO<sub>2</sub> NPs. After incubation, ROS were detected using carboxy-dichlorodihydrofluorescein diacetate (DCFDA). In addition, the side scatter signal (SSC) was monitored as a measure of TiO<sub>2</sub> particle accumulation. The data show the results from flow cytometry of a representative experiment reproduced two times with comparable results. NC, negative control; PC, positive control (100 μM H<sub>2</sub>O<sub>2</sub>).

(glutathione disulfide, GSSG) was monitored (Figure 9). After 4 h of incubation of nNHDF cells with cell culture medium only, the total cellular glutathione content was  $36.2 \pm 2.8$  or  $34.6 \pm 2.0$  nmol/mg protein in absence or presence of TiO<sub>2</sub> NPs, respectively. These values remained rather unaffected when the cells were incubated with most of the MLP ingredients but were lowered significantly when the cells were incubated with 100 μM H<sub>2</sub>O<sub>2</sub> as the positive control. However, the treatment with 0.5 mM PP in the absence of TiO<sub>2</sub> NPs and the treatment with 0.125 mM Lilial—in absence or presence of TiO<sub>2</sub> NPs—resulted in a significantly lower total cellular glutathione content (Figure 9). For Lilial, the resulting cellular glutathione contents were  $23.4 \pm 2.0$  or  $22.7 \pm 2.7$  nmol/mg protein in absence or presence of TiO<sub>2</sub> NPs, respectively. The cellular contents of GSSG remained very low (<1 nmol/mg, which is close to the detection limit of the assay) and was unaffected in all the experimental conditions.

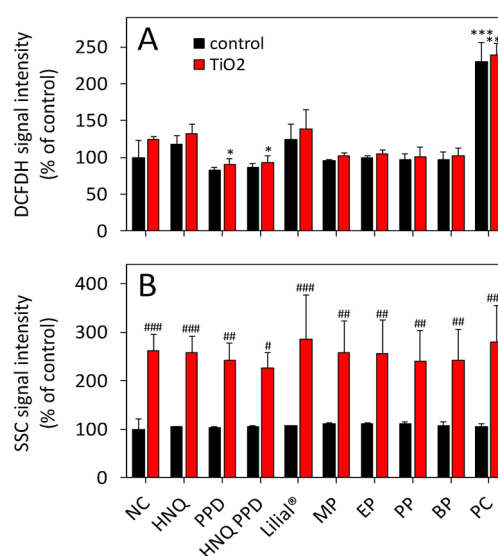


**Figure 8.** Quantification of reactive oxygen species (ROS) and particle accumulation in nNHDF cells after incubation with MLP ingredients in absence or presence of TiO<sub>2</sub> NPs. The cells were incubated for 24 h with different MLP ingredients (for concentrations see Table 1) in absence (control) or presence (TiO<sub>2</sub>) of 100 μg/mL TiO<sub>2</sub> NPs and assayed for ROS using DCFDA (A) and TiO<sub>2</sub> NP accumulation using the SSC signal intensity (B). Bar charts show median fluorescence intensities  $\pm$  SD from flow cytometry data (see Figure 7) given as percentage of negative control (NC) of three independently performed experiments. Stars indicate the significance of differences of exposed conditions compared to the negative control (NC); \* $p$  < 0.05, \*\*\* $p$  < 0.001. Hashtags indicate the significance of differences between control and TiO<sub>2</sub> NP-exposed conditions; # $p$  < 0.05, ## $p$  < 0.01, ### $p$  < 0.001. PC: positive control (100 μM H<sub>2</sub>O<sub>2</sub>).

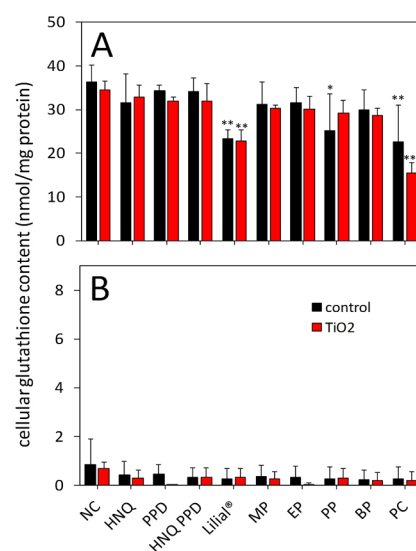


**Figure 9.** Glutathione quantification after incubation of nNHDF cells with MLP ingredients in absence or presence of TiO<sub>2</sub> NPs. The cells were incubated for 4 h with different MLP ingredients (for concentrations see Table 1) in absence (control) or presence (TiO<sub>2</sub>) of 100 μg/mL TiO<sub>2</sub> NPs, and total glutathione content (A) as well as oxidized glutathione disulfide content (B) was measured. The data represent mean values  $\pm$  SD of three independently performed experiments. Stars indicate the significance of differences of exposed conditions compared to the negative control (NC); \* $p$  < 0.05, \*\* $p$  < 0.01, \*\*\* $p$  < 0.001. PC: positive control (100 μM H<sub>2</sub>O<sub>2</sub>).

#### 4. DISCUSSION

Titanium dioxide nanoparticles (TiO<sub>2</sub> NPs) are used widely in different consumer products, including sunscreens. Although, the general view describes the skin as a tight barrier, rather impermeable to NPs, there is evidence in the recent literature that some NPs enter the *stratum corneum* or even penetrate the skin completely.<sup>9,10,14,37,38</sup>

The here used TiO<sub>2</sub> NPs were produced by a metal organic chemical vapor synthesis approach leading to pure anatase NPs without contamination with any synthesis residues or other compounds such as bacterial endotoxins (data not shown). The primary size of these particles was between 8 and 18 nm (mean: 13 nm), as reported earlier.<sup>35</sup> The fact that these particles show hydrodynamic diameters of 130 ± 13 nm indicates the formation of smaller particle agglomerates as previously published.<sup>31</sup> Agglomeration or aggregation is a frequently observed characteristic of NPs and is also known to occur for such particles in consumer products as shown for TiO<sub>2</sub> or ZnO NPs in sunscreens<sup>39</sup> or Ag NPs in antibacterial sprays.<sup>40</sup> Although it is evident that the behavior of TiO<sub>2</sub> NPs in pure H<sub>2</sub>O cannot be directly compared to the behavior in sunscreens (foams, gels, sprays, powders, etc.) the size-data obtained in this study are comparable with size-data of agglomerates found in the earlier studies of Lu and colleagues on TiO<sub>2</sub> NPs in commercial sunscreen sprays<sup>41</sup> or powders.<sup>39</sup>

Incubation of TiO<sub>2</sub> NPs with different ingredients from modern lifestyle products (MLPs) did not show severe alterations in the NP size distribution curves for most of the MLPs, suggesting no direct interaction between the substances and the particles. However, samples containing the Henna dye 2-hydroxy-1,4-naphthoquinone (HNQ) lead to an intensive change in the TiO<sub>2</sub> NP size distribution and detectable particle number, suggesting a direct interaction of this compound with the surface of the NPs. Most likely, the presence of the dye HNQ fosters the generation of larger agglomerates/aggregates of TiO<sub>2</sub> NPs that cannot be detected properly with the NTA method due to rapid gravitational settling, which would explain the reduced detectable particle number. The small fractions of smaller particles visible in the size distribution curves are likely to represent artifacts due to large glaring particles identified from the NTA video images as shown earlier for protein aggregates.<sup>42</sup> It has recently been shown, that extracts from the Henna plant *Lawsonia inermis* can be used for green synthesis of Ag or CeO<sub>2</sub> NPs,<sup>43</sup> but no study is currently available that investigates the direct interactions of HNQ with TiO<sub>2</sub> NPs. At least one study showed that HNQ extracted from Henna plants can be used to synthesize colored TiO<sub>2</sub> NPs that contain the dye and can be used for fabrication of dye-sensitized solar cells.<sup>44</sup> It should be noted furthermore that the agglomeration state of TiO<sub>2</sub> NPs influences their performance as an UV filter.<sup>45</sup>

TiO<sub>2</sub> NPs are frequently used as an UV attenuator in different skin-care products such as lotions, sunscreens, and cosmetics. Thus, the encounter of the skin to such particles and other bystander substances from the products or from MLPs used on the skin is evident, and possible combinatorial effects should be investigated. TiO<sub>2</sub> NPs alone did not result in any cytotoxicity when applied in a concentration of 100 μg/mL for 24 h. This supports earlier findings by Browning et al.<sup>46</sup> but contrasts studies of Chang et al.<sup>47</sup> who reported an EC<sub>50</sub> of 125.1 ± 23.6 μg/mL for TiO<sub>2</sub>-exposed human skin cells. The different MLP ingredients showed a classical dose-dependent

cytotoxicity with EC<sub>50</sub> values ranging from ~0.2 to 10 mM dependent on the respective substance. The highest toxicity was induced by Lilial, followed by butyl parabene and the HNQ/PPD mixture. For PPD alone, we determined an EC<sub>50</sub> of around 1 mM, which is 10 times higher than recently published data for PPD toxicity on rat skin cells.<sup>48</sup> Butyl parabene was the most toxic compound from the tested parabens followed by propyl, ethyl, and methyl parabene. This strongly suggests that the length of the side chain of the esters of 4-hydroxybenzoic acid plays a role in its cytotoxic potential. Indeed, similar findings were obtained by Lee and colleagues in a recent study on *Daphnia magna* and *Aliivibrio fischeri*.<sup>49</sup> The EC<sub>50</sub> values in this study ranged from 73.4 mg/L (0.48 mM) for methyl parabene to 2.34 mg/L (0.012 mM) for butyl parabene. A likely explanation for this fact is that parabens with longer alkyl chains have a reduced water solubility and, thus, likely a better potential for bioaccumulation.

Interestingly, the observed cytotoxicity profiles for all MLP ingredients did not change when 100 μg/mL TiO<sub>2</sub> NPs were present during the incubation. This demonstrates that there is no combinatorial (or at least no additive) effect of TiO<sub>2</sub> NPs with the different substances leading to an increase of cell death. So far, no study is available in the literature that investigates the combinatorial effects of these compounds with TiO<sub>2</sub> NPs on skin cells. In a recent paper, Roszak et al. investigated the combinatorial effects of Ag NPs with butyl parabene on human breast cell lines and concluded that there is no increased genotoxic effect of the combinatorial exposure compared to the exposure with Ag NPs alone.<sup>25</sup>

A combined apoptosis/necrosis assay was undertaken in order to investigate possible combinatorial effects between MLP ingredients and TiO<sub>2</sub> NPs in more detail. This assay also did not show any additive effects of TiO<sub>2</sub> NPs and MLP ingredients on the viability of nNHDF cells. However, we found that TiO<sub>2</sub> NP-treated cells always show a slightly higher level of PI fluorescence compared to control cells. This could be an indicator for an increased loss of membrane integrity under these conditions compared to the control. However, the data did not reach the level of significance. Furthermore, it should be noted that interferences of the TiO<sub>2</sub> NPs with the different cytotoxicity assays can also lead to the differences in the results.<sup>50</sup>

TiO<sub>2</sub> NPs have been shown to cause oxidative stress and lead to reduced cellular glutathione contents in earlier studies on human epidermal cells (A431) and human keratinocytes (HaCaT).<sup>11,51</sup> In the present study on nNHDF cells, neither TiO<sub>2</sub> NP-dependent induction of reactive oxygen species (ROS) nor a reduction in cellular glutathione content were observed. Also the used MLP ingredients did not lead to elevated ROS in nNHDF cells after incubation. HNQ and PPD even decreased the amount of detectable ROS significantly, probably due to interferences of these dyes with the used ROS indicator. Incubation of nNHDF cells with Lilial led to a significant reduction in cellular glutathione content— independently of the presence of TiO<sub>2</sub> NPs. This finding supports an earlier study by Usta and co-workers who demonstrated that HaCaT cells experience a decrease in viability and cellular ATP content and an increase in ROS production after exposure to Lilial.<sup>21</sup> The amounts of oxidized glutathione disulfide (GSSG) remained unaltered for all conditions tested, including the positive control (100 μM H<sub>2</sub>O<sub>2</sub>), which contrasts earlier findings on HaCaT cells.<sup>52</sup> A

possible explanation could be the export of oxidized GSSG from the cells as recently shown for cultured brain astrocytes.<sup>53</sup>

Significant increases in side scatter (SSC) signals in all test conditions containing TiO<sub>2</sub> NP compared to conditions without particles strongly suggest TiO<sub>2</sub> NP accumulation/uptake onto or in the cells, as shown in our earlier report on lung epithelial cells.<sup>31</sup> However, to validate these data on nNHDF cells, additional imaging techniques such as confocal laser scanning microscopy or transmission electron microscopy should be applied in future studies.

## 5. CONCLUSIONS

In summary, our data present for the first time a detailed analysis of the combinatorial effects of TiO<sub>2</sub> NPs with ingredients from modern lifestyle products (MLPs) such as Henna tattoos, skin-care products, and cosmetics. TiO<sub>2</sub> NPs alone did not cause any loss in cell viability when applied in a concentration of 100 µg/mL up to 24 h. The cytotoxicity of the different MLP ingredients exhibits typical sigmoidal dose–response relationship with EC50 values in the low millimolar range. The presence of TiO<sub>2</sub> NPs neither altered the cytotoxicity profiles of the MLP ingredients nor resulted in alterations of cellular apoptosis, ROS production, or cellular glutathione content. Taken together, it can be concluded that there are not additive effects of TiO<sub>2</sub> NPs and the selected ingredients from cosmetics or tattoos, even though the Henna tattoo ingredient 2-hydroxy-1,4-naphthoquinone (HNQ) was able to strongly influence the agglomeration behavior of the NPs. It should be noted here, that the present study only focuses on single pairwise testing of individual compounds and TiO<sub>2</sub>; whereas, the real-life situation is likely to be much more complicated, involving several compounds acting together and (potentially) interacting with NPs. We suggest that similar studies should be part of the safety analysis of consumer products when it can be expected that use of an NP-enabled product leads to coexposure with potentially problematic chemicals.

## AUTHOR INFORMATION

### Corresponding Author

**Mark Geppert** – Department of Biosciences and Allergy Cancer Bio Nano Research Centre, University of Salzburg 5020 Salzburg, Austria; [orcid.org/0000-0001-6684-2508](https://orcid.org/0000-0001-6684-2508)

### Authors

**Alexandra Schwarz** – Department of Biosciences and Allergy Cancer Bio Nano Research Centre, University of Salzburg 5020 Salzburg, Austria

**Lea Maria Stangassinger** – Department of Biosciences and Allergy Cancer Bio Nano Research Centre, University of Salzburg 5020 Salzburg, Austria

**Susanna Wenger** – Department of Biosciences and Allergy Cancer Bio Nano Research Centre, University of Salzburg 5020 Salzburg, Austria

**Lisa Maria Wienerroither** – Department of Biosciences and Allergy Cancer Bio Nano Research Centre, University of Salzburg 5020 Salzburg, Austria

**Stefanie Ess** – Department of Biosciences and Allergy Cancer Bio Nano Research Centre, University of Salzburg 5020 Salzburg, Austria

**Albert Duschl** – Department of Biosciences and Allergy Cancer Bio Nano Research Centre, University of Salzburg 5020 Salzburg, Austria; [orcid.org/0000-0002-7034-9860](https://orcid.org/0000-0002-7034-9860)

**Martin Himly** – Department of Biosciences and Allergy Cancer Bio Nano Research Centre, University of Salzburg 5020 Salzburg, Austria; [orcid.org/0000-0001-5416-085X](https://orcid.org/0000-0001-5416-085X)

Complete contact information is available at:  
<https://pubs.acs.org/10.1021/acs.chemrestox.9b00428>

## Notes

The authors declare no competing financial interest.

## ACKNOWLEDGMENTS

This work was funded by the Sparkling Science project “Nano-Style”, grant no. SPA06/270 of the Austrian Federal Ministry of Education, Science and Research (BMBWF).

## LIST OF ABBREVIATIONS

2-VP	2-vinylpyridine
ANOVA	analysis of variances
ATP	adenosine triphosphate
BB	binding buffer
BP	butyl parabene
CTB	CellTiter-Blue
DCFDA	2',7'-dichlorodihydrofluorescein diacetate
DMEM	Dulbecco's modified Eagle's Medium
DMSO	dimethyl sulfoxide
DTNB	5,5'-dithiobis(2-nitrobenzoic acid)
EDTA	ethylenediaminetetraacetic acid
EP	ethyl parabene
FBS	fetal bovine serum
FITC	fluorescein isothiocyanate
GSH	glutathione
GSSG	glutathione disulfide
HEPES	4-(2-hydroxyethyl)-1-piperazineethanesulfonic acid
HNQ	2-hydroxy-1,4-naphthoquinone
MLP	modern lifestyle product
MP	methyl parabene
NADPH	nicotinamide adenine dinucleotide phosphate
NC	negative control
nNHDF	neonatal normal human dermal fibroblasts
NP	nanoparticle
NRU	Neutral Red uptake
NTA	nanoparticle tracking analysis
PBS	phosphate buffered saline
PC	positive control
PI	propidium iodide
PP	propyl parabene
PPD	para-phenylenediamine
ROS	reactive oxygen species
SD	standard deviation
SSA	sulfosalicylic acid
SSC	side scatter
UV	ultraviolet

## REFERENCES

- (1) Bondarenko, O.; Juganson, K.; Ivask, A.; Kasemets, K.; Mortimer, M., and Kahru, A. (2013) Toxicity of Ag, CuO and ZnO nanoparticles to selected environmentally relevant test organisms and mammalian cells in vitro: a critical review. *Arch. Toxicol.* 87, 1181–1200.
- (2) Piccinno, F., Gottschalk, F., Seeger, S., and Nowack, B. (2012) Industrial production quantities and uses of ten engineered nanomaterials in Europe and the world. *J. Nanopart. Res.* 14.
- (3) McSweeney, P. C. (2016) The safety of nanoparticles in sunscreens: An update for general practice. *Aust Fam Physician* 45, 397–399.

- (4) Newman, M. D., Stotland, M., and Ellis, J. I. (2009) The safety of nanosized particles in titanium dioxide- and zinc oxide-based sunscreens. *J. Am. Acad. Dermatol.* 61, 685–692.
- (5) Sadrieh, N., Wokovich, A. M., Gopee, N. V., Zheng, J., Haines, D., Parmiter, D., Siitonen, P. H., Cozart, C. R., Patri, A. K., McNeil, S. E., Howard, P. C., Doub, W. H., and Buhse, L. F. (2010) Lack of significant dermal penetration of titanium dioxide from sunscreen formulations containing nano- and submicron-size TiO<sub>2</sub> particles. *Toxicol. Sci.* 115, 156–166.
- (6) Shakeel, M., Jabeen, F., Shabbir, S., Asghar, M. S., Khan, M. S., and Chaudhry, A. S. (2016) Toxicity of Nano-Titanium Dioxide (TiO<sub>2</sub>-NP) Through Various Routes of Exposure: a Review. *Biol. Trace Elem. Res.* 172, 1–36.
- (7) Crosera, M., Prodi, A., Mauro, M., Pelin, M., Florio, C., Bellomo, F., Adami, G., Apostoli, P., De Palma, G., Bovenzi, M., Campanini, M., and Filon, F. L. (2015) Titanium Dioxide Nanoparticle Penetration into the Skin and Effects on HaCaT Cells. *Int. J. Environ. Res. Public Health* 12, 9282–9297.
- (8) Xie, G., Lu, W., and Lu, D. (2015) Penetration of titanium dioxide nanoparticles through slightly damaged skin in vitro and in vivo. *J. Appl. Biomater. Funct. Mater.* 13, e356–361.
- (9) Wu, J., Liu, W., Xue, C., Zhou, S., Lan, F., Bi, L., Xu, H., Yang, X., and Zeng, F. D. (2009) Toxicity and penetration of TiO<sub>2</sub> nanoparticles in hairless mice and porcine skin after subchronic dermal exposure. *Toxicol. Lett.* 191, 1–8.
- (10) Pelclova, D., Navratil, T., Kacerova, T., Zamostna, B., Fenclova, Z., Vlckova, S., and Kacer, P. (2019) NanoTiO<sub>2</sub> Sunscreen Does Not Prevent Systemic Oxidative Stress Caused by UV Radiation and a Minor Amount of NanoTiO<sub>2</sub> is Absorbed in Humans. *Nanomaterials* 9, 888.
- (11) Wright, C., Iyer, A. K., Wang, L., Wu, N., Yakisich, J. S., Rojanasakul, Y., and Azad, N. (2017) Effects of titanium dioxide nanoparticles on human keratinocytes. *Drug Chem. Toxicol.* 40, 90–100.
- (12) Pan, Z., Lee, W., Slutsky, L., Clark, R. A., Pernodet, N., and Rafailovich, M. H. (2009) Adverse effects of titanium dioxide nanoparticles on human dermal fibroblasts and how to protect cells. *Small* 5, 511–520.
- (13) Horie, M., Sugino, S., Kato, H., Tabei, Y., Nakamura, A., and Yoshida, Y. (2016) Does photocatalytic activity of TiO<sub>2</sub> nanoparticles correspond to photo-cytotoxicity? Cellular uptake of TiO<sub>2</sub> nanoparticles is important in their photo-cytotoxicity. *Toxicol. Mech. Methods* 26, 284–294.
- (14) Smijs, T. G., and Pavel, S. (2011) Titanium dioxide and zinc oxide nanoparticles in sunscreens: focus on their safety and effectiveness. *Nanotechnol., Sci. Appl.* 4, 95–112.
- (15) Diepgen, T. L., Naldi, L., Bruze, M., Cazzaniga, S., Schuttelaar, M. L., Elsner, P., Goncalo, M., Ofenloch, R., and Svensson, A. (2016) Prevalence of Contact Allergy to p-Phenylenediamine in the European General Population. *J. Invest. Dermatol.* 136, 409–415.
- (16) Panfili, E., Esposito, S., and Di Cara, G. (2017) Temporary Black Henna Tattoos and Sensitization to para-Phenylenediamine (PPD): Two Paediatric Case Reports and a Review of the Literature. *Int. J. Environ. Res. Public Health* 14, 421.
- (17) Calogiuri, G., Di Leo, E., Butani, L., Pizzimenti, S., Incorvaia, C., Macchia, L., and Nettis, E. (2017) Hypersensitivity reactions due to black henna tattoos and their components: are the clinical pictures related to the immune pathomechanism? *Clin. Mol. Allergy* 15, 8.
- (18) Lee, O. K., Cha, H. J., Lee, M. J., Lim, K. M., Jung, J. W., Ahn, K. J., An, I. S., An, S., and Bae, S. (2015) Implication of microRNA regulation in para-phenylenediamine-induced cell death and senescence in normal human hair dermal papilla cells. *Mol. Med. Rep.* 12, 921–936.
- (19) Arnau, E. G., Andersen, K. E., Bruze, M., Frosch, P. J., Johansen, J. D., Menne, T., Rastogi, S. C., White, I. R., and Lepoittevin, J. P. (2000) Identification of Liliat (R) as a fragrance sensitizer in a perfume by bioassay-guided chemical fractionation and structure-activity relationships. *Contact Dermatitis* 43, 351–358.
- (20) Larsen, W. G. (1983) Allergic contact dermatitis to the fragrance material liliat. *Contact Dermatitis* 9, 158–159.
- (21) Usta, J., Hachem, Y., El-Rifai, O., Bou-Moughlabey, Y., Echtay, K., Griffiths, D., Nakkash-Chmisse, H., and Makki, R. F. (2013) Fragrance chemicals lylal and liliat decrease viability of HaCat cells<sup>†</sup> by increasing free radical production and lowering intracellular ATP level: protection by antioxidants. *Toxicol. In Vitro* 27, 339–348.
- (22) Bledzka, D., Gromadzinska, J., and Wasowicz, W. (2014) Parabens. From environmental studies to human health. *Environ. Int.* 67, 27–42.
- (23) Darbre, P. D., and Harvey, P. W. (2008) Paraben esters: review of recent studies of endocrine toxicity, absorption, esterase and human exposure, and discussion of potential human health risks. *J. Appl. Toxicol.* 28, 561–578.
- (24) Nakagawa, Y., and Moldeus, P. (1998) Mechanism of p-hydroxybenzoate ester-induced mitochondrial dysfunction and cytotoxicity in isolated rat hepatocytes. *Biochem. Pharmacol.* 55, 1907–1914.
- (25) Roszak, J., Domeradzka-Gajda, K., Smok-Pieniazek, A., Kozajda, A., Spryszynska, S., Grobelny, J., Tomaszewska, E., Ranoszek-Soliwoda, K., Cieslak, M., Puchowicz, D., and Stepnik, M. (2017) Genotoxic effects in transformed and non-transformed human breast cell lines after exposure to silver nanoparticles in combination with aluminium chloride, butylparaben or di-n-butylphthalate. *Toxicol. In Vitro* 45, 181–193.
- (26) Elser, M. J., Berger, T., Brandhuber, D., Bernardi, J., Diwald, O., and Knozinger, E. (2006) Particles coming together: electron centers in adjoined TiO<sub>2</sub> nanocrystals. *J. Phys. Chem. B* 110, 7605–7608.
- (27) Marquez, A., Berger, T., Feinle, A., Husing, N., Himly, M., Duschl, A., and Diwald, O. (2017) Bovine Serum Albumin Adsorption on TiO<sub>2</sub> Colloids: The Effect of Particle Agglomeration and Surface Composition. *Langmuir* 33, 2551–2558.
- (28) Marquez, A., Kocsis, K., Zickler, G., Bourret, G. R., Feinle, A., Husing, N., Himly, M., Duschl, A., Berger, T., and Diwald, O. (2017) Enzyme adsorption-induced activity changes: a quantitative study on TiO<sub>2</sub> model agglomerates. *J. Nanobiotechnol.* 15, 55.
- (29) Mayring, P. (2010) *Qualitative Inhaltsanalyse: Grundlagen und Techniken*, Beltz, Weinheim/Basel.
- (30) Filipe, V., Hawe, A., and Jiskoot, W. (2010) Critical evaluation of Nanoparticle Tracking Analysis (NTA) by NanoSight for the measurement of nanoparticles and protein aggregates. *Pharm. Res.* 27, 796–810.
- (31) Grotz, B., Geppert, M., Mills-Goodlet, R., Hofer, S., Hofstätter, N., Asam, C., Feinle, A., Kocsis, K., Berger, T., and Diwald, O. (2018) Biologic effects of nanoparticle-allergen conjugates: time-resolved uptake using an in vitro lung epithelial co-culture model of A549 and THP-1 cells. *Environ. Sci.: Nano* 5, 2184–2197.
- (32) Crowley, L. C., Marfell, B. J., Scott, A. P., and Waterhouse, N. J. (2016) Quantitation of Apoptosis and Necrosis by Annexin V Binding, Propidium Iodide Uptake, and Flow Cytometry. *Cold Spring Harb Protoc* 2016, pdb.prot087288.
- (33) Tietze, F. (1969) Enzymic method for quantitative determination of nanogram amounts of total and oxidized glutathione: applications to mammalian blood and other tissues. *Anal. Biochem.* 27, 502–522.
- (34) Lowry, O. H., Rosebrough, N. J., Farr, A. L., and Randall, R. J. (1951) Protein measurement with the Folin phenol reagent. *J. Biol. Chem.* 193, 265–275.
- (35) Berger, T., Sterrer, M., Diwald, O., and Knozinger, E. (2005) Charge trapping and photoadsorption of O<sub>2</sub> on dehydroxylated TiO<sub>2</sub> nanocrystals—an electron paramagnetic resonance study. *ChemPhysChem* 6, 2104–2112.
- (36) Zucker, R. M., Massaro, E. J., Sanders, K. M., Degn, L. L., and Boyes, W. K. (2010) Detection of TiO<sub>2</sub> nanoparticles in cells by flow cytometry. *Cytometry, Part A* 77, 677–685.
- (37) Mortensen, L. J., Oberdorster, G., Pentland, A. P., and Delouise, L. A. (2008) In vivo skin penetration of quantum dot nanoparticles in the murine model: the effect of UVR. *Nano Lett.* 8, 2779–2787.

(38) Rancan, F., Gao, Q., Graf, C., Troppens, S., Hadam, S., Hackbarth, S., Kembuan, C., Blume-Peytavi, U., Ruhl, E., Lademann, J., and Vogt, A. (2012) Skin penetration and cellular uptake of amorphous silica nanoparticles with variable size, surface functionalization, and colloidal stability. *ACS Nano* 6, 6829–6842.

(39) Lu, P. J., Fang, S. W., Cheng, W. L., Huang, S. C., Huang, M. C., and Cheng, H. F. (2018) Characterization of titanium dioxide and zinc oxide nanoparticles in sunscreen powder by comparing different measurement methods. *J. Food Drug Anal* 26, 1192–1200.

(40) Tulve, N. S., Stefaniak, A. B., Vance, M. E., Rogers, K., Mwilu, S., LeBouf, R. F., Schwegler-Berry, D., Willis, R., Thomas, T. A., and Marr, L. C. (2015) Characterization of silver nanoparticles in selected consumer products and its relevance for predicting children's potential exposures. *Int. J. Hyg. Environ. Health* 218, 345–357.

(41) Lu, P. J., Cheng, W. L., Huang, S. C., Chen, Y. P., Chou, H. K., and Cheng, H. F. (2015) Characterizing titanium dioxide and zinc oxide nanoparticles in sunscreen spray. *Int. J. Cosmet. Sci.* 37, 620–626.

(42) Tian, X., Nejadnik, M. R., Baunsgaard, D., Henriksen, A., Rischel, C., and Jiskoot, W. (2016) A Comprehensive Evaluation of Nanoparticle Tracking Analysis (NanoSight) for Characterization of Proteinaceous Submicron Particles. *J. Pharm. Sci.* 105, 3366–3375.

(43) Kalakotla, S., Jayarambabu, N., Mohan, G. K., Mydin, R., and Gupta, V. R. (2019) A novel pharmacological approach of herbal mediated cerium oxide and silver nanoparticles with improved biomedical activity in comparison with Lawsonia inermis. *Colloids Surf., B* 174, 199–206.

(44) Ananth, S., Vivek, P., Arumanayagam, T., and Murugakoothan, P. (2014) Natural dye extract of lawsonia inermis seed as photo sensitizer for titanium dioxide based dye sensitized solar cells. *Spectrochim. Acta, Part A* 128, 420–426.

(45) Tyner, K. M., Wokovich, A. M., Godar, D. E., Doub, W. H., and Sadrieh, N. (2011) The state of nano-sized titanium dioxide (TiO<sub>2</sub>) may affect sunscreen performance. *Int. J. Cosmet. Sci.* 33, 234–244.

(46) Browning, C. L., The, T., Mason, M. D., and Wise, J. P., Sr. (2014) Titanium Dioxide Nanoparticles are not Cytotoxic or Clastogenic in Human Skin Cells. *J. Environ. Anal Toxicol.* 4.

(47) Chang, J., Lee, C. W., Alsulimani, H. H., Choi, J. E., Lee, J. K., Kim, A., Park, B. H., Kim, J., and Lee, H. (2016) Role of fatty acid composites in the toxicity of titanium dioxide nanoparticles used in cosmetic products. *J. Toxicol. Sci.* 41, 533–542.

(48) Seydi, E., Fatahi, M., Naserzadeh, P., and Pourahmad, J. (2019) The effects of para-phenylenediamine (PPD) on the skin fibroblast cells. *Xenobiotica* 49, 1143–1148.

(49) Lee, J., Bang, S. H., Kim, Y. H., and Min, J. (2018) Toxicities of Four Parabens and Their Mixtures to *Daphnia magna* and *Aliivibrio fischeri*. *Environ. Health Toxicol* 33, No. e2018018.

(50) Guadagnini, R., Halamoda Kenzaoui, B., Walker, L., Pojana, G., Magdolenova, Z., Bilanicova, D., Saunders, M., Juillerat-Jeanneret, L., Marcomini, A., Huk, A., Dusinska, M., Fjellsbo, L. M., Marano, F., and Boland, S. (2015) Toxicity screenings of nanomaterials: challenges due to interference with assay processes and components of classic in vitro tests. *Nanotoxicology* 9, 13–24.

(51) Shukla, R. K., Sharma, V., Pandey, A. K., Singh, S., Sultana, S., and Dhawan, A. (2011) ROS-mediated genotoxicity induced by titanium dioxide nanoparticles in human epidermal cells. *Toxicol. In Vitro* 25, 231–241.

(52) Inbaraj, J. J., and Chignell, C. F. (2004) Cytotoxic action of juglone and plumbagin: a mechanistic study using HaCaT keratinocytes. *Chem. Res. Toxicol.* 17, 55–62.

(53) Steinmeier, J., and Dringen, R. (2019) Exposure of Cultured Astrocytes to Menadione Triggers Rapid Radical Formation, Glutathione Oxidation and Mrp1-Mediated Export of Glutathione Disulfide. *Neurochem. Res.* 44, 1167–1181.